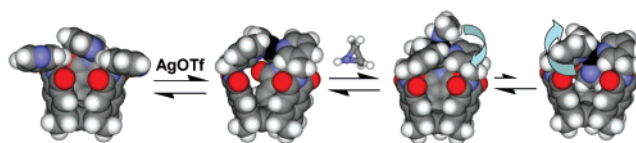


Silver(I) Mediated Folding of a Molecular  
BasketZhiqing Yan, Shijing Xia, Matthew Gardlik, Wanji Seo, Veselin Maslak,  
Judith Gallucci, Christopher M. Hadad, and Jovica D. Badjić\**Department of Chemistry, The Ohio State University, 100 West 18th Avenue,  
Columbus, Ohio 43210**badjic@chemistry.ohio-state.edu*

Received March 6, 2007

## ABSTRACT



We have investigated Ag(I) mediated folding of a tridentate compound, containing three pyridine flaps tethered to a semirigid scaffold, into a molecular basket, using both experimental and theoretical methods. The basket formation has been shown to be highly favorable in organic media ( $\Delta G^\circ = -7.2$  kcal/mol), with the assembly process allowing for another ligand to bind preferentially on the outer side.

Molecular receptors containing a cavity and capable of recognizing guests on the basis of their shape, size, and functionality<sup>1</sup> have been of great interest for studying transient intermediates,<sup>2</sup> catalysis,<sup>3</sup> molecular encapsulation,<sup>4</sup> and new forms of stereoisomerism.<sup>5</sup> Our research program, oriented toward developing a family of molecular baskets<sup>6</sup> and cavitands with allosterically controllable conformational dynamics<sup>7</sup> to allow for the regulation of molecular recognition and reactivity, has been largely inspired by the natural world.<sup>8</sup> In this study, we report on the experimental preparation and characterization, along with a theoretical investiga-

tion, of the conformational dynamics and recognition behavior of Ag(I) containing molecular basket **6** (Figures 1

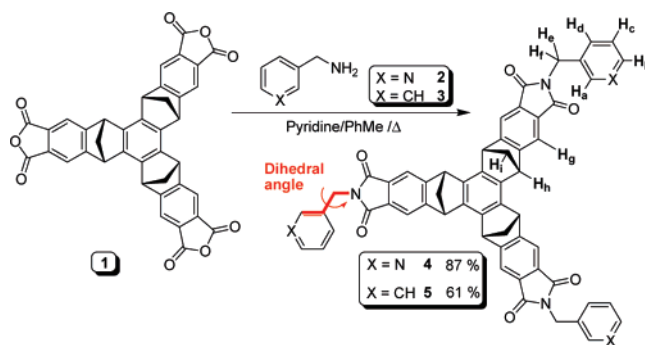


**Figure 1.** Synthesis of polydentate **4** and model compound **5**.

and 2). Our study reveals the prospect of using a transition metal to enclose space by bringing together ligands appended to a tridentate bowl-shaped host, thereby allowing the coordinatively unsaturated metal to further bind another molecule by placing it inside or outside the cavity. The encapsulation and detection of target molecules in such hosts

(1) (a) Cram, D. J.; Cram, J. M. In *Container Molecules and Their Guests*; The RSC: Cambridge, UK, 1994. (b) Jasat, A.; Sherman, J. C. *Chem. Rev.* **1999**, *99*, 931. (c) Hof, F.; Craig, S. L.; Nuckolls, C.; Rebek, J., Jr. *Angew. Chem., Int. Ed.* **2002**, *41*, 1488.

(2) (a) Warmuth, R. *Eur. J. Org. Chem.* **2001**, *3*, 423. (b) Zyryanov, G. V.; Rudkevich, D. M. *Org. Lett.* **2003**, *5*, 1253. (c) Dong, V. M.; Fiedler, D.; Carl, B.; Bergman, R. G. *J. Am. Chem. Soc.* **2006**, *128*, 14464.

(3) (a) Yoshizawa, M.; Tamura, M.; Fujita, M. *Science* **2006**, *312*, 251. (b) Leung, D. H.; Bergman, R. G.; Raymond, K. N. *J. Am. Chem. Soc.* **2006**, *128*, 9781.

(4) (a) Gibb, C. L. D.; Gibb, B. C. *J. Am. Chem. Soc.* **2004**, *126*, 11408. (b) Fox, O. D.; Cookson, J.; Wilkinson, E. J. S.; Drew, M. G. B.; MacLean, E. J.; Teat, S. J.; Beer, P. D. *J. Am. Chem. Soc.* **2006**, *128*, 6990.

(5) Scarso, A.; Shivanyuk, A.; Hayashida, O.; Rebek, J., Jr. *J. Am. Chem. Soc.* **2003**, *125*, 6239.

(6) Maslak, V.; Yan, Z.; Xia, S.; Gallucci, J.; Hadad, C. M.; Badjić, J. D. *J. Am. Chem. Soc.* **2006**, *128*, 5887. For the synthesis, see also: Durr, R.; Cossu, S.; Lucchini, V.; De Lucchi, O. *Angew. Chem., Int. Ed.* **1998**, *36*, 2805.

(7) Yan, Z.; Chang, Y.; Mayo, D.; Maslak, V.; Xia, S.; Badjić, J. D. *Org. Lett.* **2006**, *8*, 3697.

(8) Zhou, H.-X.; Wlodek, S. T.; McCammon, J. A. *Proc. Natl. Acad. Sci.* **1998**, *95*, 9280.

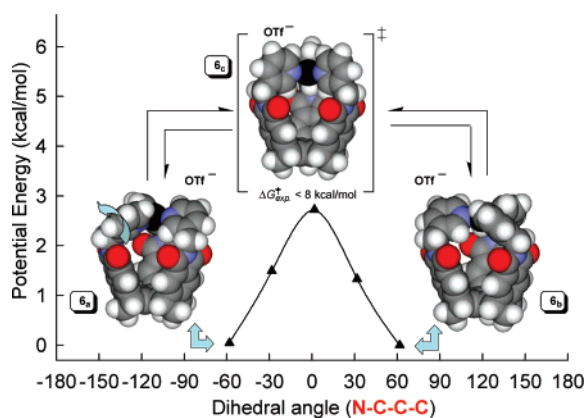


**Figure 2.** Energy minimized (DFT, BP86) conformations of **6<sub>a</sub>**, **6<sub>b</sub>**, and **6<sub>c</sub>**; calculated potential energy diagram for **6<sub>a</sub>**/**6<sub>b</sub>** interconversion via synchronized rotation of pyridine flaps about their N–C–C–C dihedral angle.

could be greatly facilitated by means of coordination,<sup>9</sup> while new strategies for regulating chemical reactivity in dynamic, confined environments can also be developed. The synthesis of **4** (Figure 1) followed the originally reported methodology for the preparation of **5**.<sup>6</sup> The amidation step, whereby the corresponding trianhydride **1** was reacted with 3-(amino-methyl)pyridine **2** in toluene, was fraught with difficulties. The presence of external pyridine as a co-reactant was found to have a dramatic effect on the formation of **4**: the reaction proceeded with a catalytic amount but not with an excess or in the absence of pyridine (Figure 1).

With the aid of <sup>1</sup>H–<sup>1</sup>H COSY and NOESY two-dimensional experiments,<sup>10</sup> the <sup>1</sup>H NMR spectrum of **4** (CDCl<sub>3</sub>/CD<sub>3</sub>OD, 1:1) was assigned to a molecule with averaged C<sub>3v</sub> symmetry (Figures 1 and 3a). Incremental additions of AgOTf to its solution prompted considerable <sup>1</sup>H NMR spectroscopic changes (Figure 3): the signal for the H<sub>a</sub> proton shifted upfield ( $\Delta\delta_{\max} = 0.46$  ppm), while the resonances for the H<sub>c/d</sub> protons shifted downfield ( $\Delta\delta_{\max} = 0.23$  and 0.21 ppm, respectively). The spectroscopic changes were persistent until the 1:1 ratio of Ag(I):**4** was reached (Figure 3k); additional quantities of AgOTf had no considerable effects on the <sup>1</sup>H NMR spectrum. Notably, a single set of peaks with the originally observed C<sub>3v</sub> symmetrical appearance, corresponding to all equilibrating species in solution, remained during the titration. In a control experiment, incremental addition of AgOTf (1.4 equiv) to **5**, containing three benzene flaps incapable of interacting strongly with Ag(I), caused no observable changes in its <sup>1</sup>H NMR spectrum.<sup>10</sup>

The results of the titration experiments thus suggest the formation of chelated **6** (Figure 2), which is exchanging rapidly with **4** and AgOTf on the NMR time scale. Nonlinear least-squares analysis of the titration data suggested an apparent stability constant for the formation of **6** to be greater than 10<sup>4</sup> M<sup>-1</sup>.<sup>10</sup>

(9) (a) Wallace, K. J.; Belcher, W. J.; Turner, D. R.; Syed, K. F.; Steed, J. W. *J. Am. Chem. Soc.* **2003**, *125*, 9699. (b) Kang, O.; Hossain, M. A.; Bowman-James, K. *Coord. Chem. Rev.* **2006**, *250*, 3038.

(10) See the Supporting Information for more details.

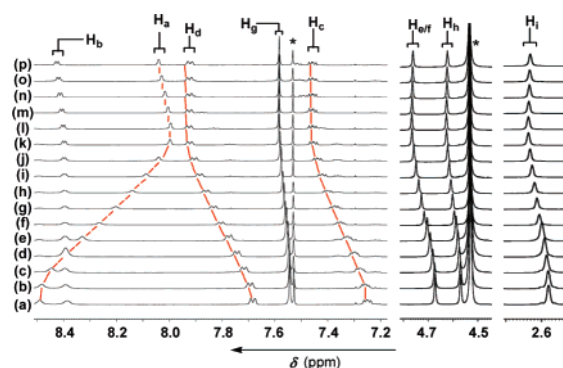


**Figure 3.** A series of <sup>1</sup>H NMR spectra (500 MHz, 298 K, CDCl<sub>3</sub>/CD<sub>3</sub>OD, 1:1) of **4** (5.4 mM), recorded on addition of a 124.0 mM standard solution of AgOTf (CDCl<sub>3</sub>/CD<sub>3</sub>OD, 1:1) such that the final mixture comprises (a) 0, (b) 0.1, (c) 0.2, (d) 0.3, (e) 0.4, (f) 0.5, (g) 0.6, (h) 0.7, (i) 0.8, (j) 0.9, (k) 1.0, (l) 1.2, (m) 1.4, (n) 1.6, (o) 1.8, and (p) 2.0 mol equiv of AgOTf.

The high affinity of Ag(I) toward polydentate **4** was corroborated by a MALDI-TOF mass spectrometric experiment whereby the exclusive appearance of a peak at 1007.3 amu, corresponding to [4:Ag]<sup>+</sup> = [6-OTf]<sup>+</sup> cation, was observed.<sup>10</sup> 2D DOSY (<sup>1</sup>H NMR)<sup>11</sup> experiments also pointed to the formation of **6**: The hydrodynamic radii of **6** (6.7 ± 0.1 Å) and **4** (7.4 ± 0.2 Å) were obtained by using their diffusion coefficients, i.e., estimated on the basis of modified Stokes–Einstein and Grunberg equations.<sup>11b</sup> Evidently, the binding of Ag(I) to **4** caused its folding, which reduced its effective volume and increased the apparent translational mobility. On the basis of MALDI-TOF and DOSY experiments, the absence of intermolecular aggregates, potentially developed in the assembly process, was also verified.

Thermodynamic parameters for the formation of **6** were obtained more accurately by isothermal titration calorimetry (ITC, Figure 4). The experiments showed that the assembly process (300 K, CHCl<sub>3</sub>/CH<sub>3</sub>OH, 1:1) is endothermic ( $\Delta H^\circ = 3.0 \pm 0.1$  kcal/mol). The fitting procedure revealed  $K_a = (1.9 \pm 0.3) \times 10^5$  M<sup>-1</sup> ( $\Delta G^\circ = -7.2$  kcal/mol) and  $n = 1.28$  (stoichiometric proportion) as independently fit parameters. Thus, the association of **4** and AgOTf into **6** is strongly entropy-driven ( $\Delta S^\circ = 34$  eu). The stepwise formation of Ag(pyridine)<sub>2</sub><sup>+</sup> has, however, been shown to be enthalpically favored and entropically disfavored ( $\Delta H^\circ = -11.2 \pm 0.1$  kcal/mol;  $\Delta S^\circ = -18.9 \pm 0.4$  eu).<sup>12</sup> It thus appears that the entropic advantage in the formation of **6** was likely developed by way of the chelate effect operating in its assembly.<sup>13b,c</sup> Reorganization of the solvent shell, resulting from the differential solvation in the course of the complexation, may have also contributed to the effect.<sup>13a</sup>

(11) (a) Cohen, Y.; Avram, L.; Frish, L. *Angew. Chem., Int. Ed.* **2005**, *44*, 520. (b) Zuccaccia, D.; Pironcini, L.; Pinalli, R.; Dalcanale, E.; Macchioni, A. *J. Am. Chem. Soc.* **2005**, *127*, 7025.

(12) Izatt, R. M.; Eatough, D.; Snow, R. L.; Christensen, J. J. *J. Phys. Chem.* **1968**, *72*, 1208.

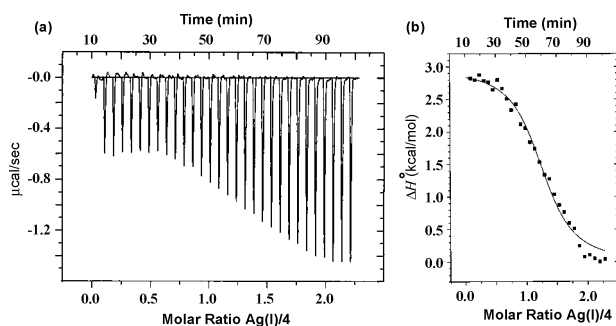


**Figure 4.** (a) Isothermal titration calorimetry (ITC) data for the titration of a solution of **4** (0.1 mM, 300  $\mu$ L) with a 1.0 mM standard solution of AgOTf ( $\text{CDCl}_3/\text{CD}_3\text{OD} = 1:1$ ) at 300 K. (b) Computer simulated curve fitting afforded the thermodynamic parameters for the assembly.

Density functional theory (DFT, BP86 functional) calculations<sup>14</sup> of the optimized geometries of **6** show that the three pyridine moieties, coordinated to Ag(I), are twisted in the same direction with a propeller-like geometry, and with either a *P* or *M* sense of twist (Figure 2). In consequence, the molecule flutters between two enantiomeric forms **6<sub>a</sub>**/**6<sub>b</sub>** by a synchronized rotation of the pyridine flaps, with a calculated activation barrier of only 2.7 kcal/mol. Indeed, 2D NMR NOESY spectroscopic measurements of **6** (1.4 mM,  $\text{CDCl}_3/\text{CD}_3\text{OD}$ , 1:1) revealed a **H<sub>a</sub>**/**H<sub>b</sub>** NOE cross-peak (Figure 5), indicating a spatial proximity of the flaps

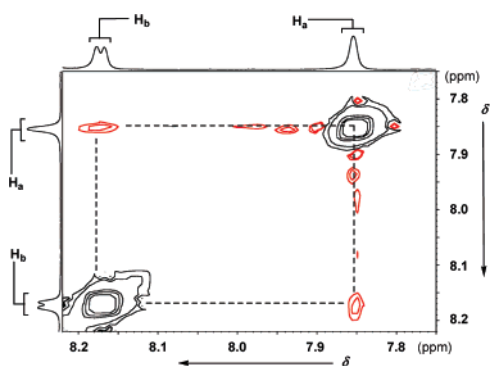


**Figure 5.** Selected region of the  $^1\text{H}$ – $^1\text{H}$  NOESY NMR spectrum of **6** (500 MHz,  $\text{CDCl}_3/\text{CD}_3\text{OD} = 1:1$ , 1.36 mM, 300 K) revealing the **H<sub>a</sub>**/**H<sub>b</sub>** correlation through space.

(through-space distance of two proton nuclei  $< 4.5 \text{ \AA}$ ).<sup>15</sup> The same NOE correlation was, however, not observed for **4** itself. Additionally, variable-temperature  $^1\text{H}$  NMR studies of **6** showed broadening of the resonances at low tempera-

tures.<sup>10</sup> A complete decoalescence for **H<sub>e</sub>**/**H<sub>f</sub>** signals was, however, not observed even at 183 K ( $\text{CD}_2\text{Cl}_2/\text{CD}_3\text{COD}$ , 9:1), suggesting a low activation barrier ( $\Delta G^\ddagger$  less than 8 kcal/mol) for the **6<sub>a/b</sub>** interconversion. This is in agreement with the results of our theoretical calculations (Figure 2).

In the course of our studies, we attempted to observe the encapsulation of various molecules in **6** (not coordinated to Ag(I)) at ambient and lower temperatures. Supposedly, the dynamic and “folded interior” of **6** prevented the incarceration of a guest with affinity high enough to be observed with  $^1\text{H}$  NMR spectroscopy. A single-crystal X-ray study of **7** (Figure 6a),<sup>10</sup> however, revealed an ordered molecule of

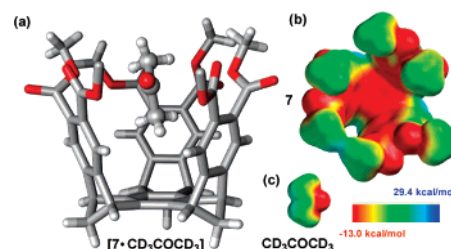


**Figure 6.** (a) Ball and stick representation of the structure of the  $[\mathbf{7} \cdot \text{CH}_3\text{C}(=\text{O})\text{CH}_3]$  complex in the solid state (some hydrogens are omitted for clarity). (b, c) Electrostatic potential surface maps of **7** and  $\text{CD}_3\text{COCD}_3$ , respectively, calculated by using the AM1 method by Spartan Software.

acetone positioned inside this cavitand and along its  $\text{C}_3$  axis. The  $\text{C}-\text{H} \cdots \pi$  interaction could be responsible for the assembly in the solid state,<sup>16</sup> as the buried  $\text{CH}_3$  group faces the surrounding aromatic rings. On the basis of a CSD crystallographic database search, the  $\text{C}-\text{H} \cdots \pi$  centroid distance was estimated to be about 2.91  $\text{\AA}$ ,<sup>16–17</sup> which in the case of  $[\mathbf{7} \cdot \text{CH}_3\text{C}(=\text{O})\text{CH}_3]$  is slightly beyond that range (2.87–3.36  $\text{\AA}$ , Figure 6a). The complementary electrostatic surfaces (Figure 6b,c) in combination with crystal packing can also contribute to the formation of the clathrate.<sup>18</sup> Supposedly, Ag(I) in **6** is weakly bound to the triflate counterion or methanol so as to benefit from full coordination. We reasoned that addition of a “good” monodentate ligand would displace the labile one, and allow the formation of a coordination complex in which the guest is situated either outside or inside the basket cavity (137  $\text{\AA}^3$  in volume; Figure 8). DFT (BP86) calculations have shown that the binding of appropriately sized guests **8–12** to **6** is somewhat favored on the outside ( $\Delta\Delta E_p = 2.1$  to 6.1 kcal/mol, Figure 8). Moreover, a small activation energy for complexation/decomplexation of solvent molecules  $\text{CHCl}_3$  and  $\text{CH}_3\text{OH}$  has

(15) Scheerder, J.; Vreekamp, R. H.; Engbersen, J. F. J.; Verboom, W.; van Duynhoven, J. P. M.; Reinhoudt, D. N. *J. Org. Chem.* **1996**, *61*, 3476.

(16) Nishio, M.; Hirota, M.; Umezawa, Y. In *CH/π Interaction: Evidence, Nature, and Consequences*; Wiley-VCH: Weinheim, Germany, 1998.

(17) Takemura, H.; Iwanaga, T.; Shimmyozu, T. *Tetrahedron Lett.* **2005**, *46*, 6687.

(18) Dalgarno; Thallapally, S. J. P. K.; Barbour, L. J.; Atwood, J. L. *Chem. Soc. Rev.* **2007**, *36*, 236.

(13) (a) Berger, M.; Schmidtchen, F. P. *Angew. Chem., Int. Ed.* **1998**, *37*, 2694. (b) Badjić, J. D.; Nelson, A.; Cantrill, S. J.; Turnbull, W. B.; Stoddart, J. F. *Acc. Chem. Res.* **2005**, *38*, 723. (c) Bea, I.; Gotsev, M. G.; Ivanov, P. M.; Jaime, C.; Kollman, P. A. *J. Org. Chem.* **2006**, *71*, 2056.

(14) (a) Perdew, J. P. *Phys. Rev. B* **1986**, *33*, 8822. (b) Becke, A. D. *Phys. Rev. A* **1998**, *38*, 3098.

also been calculated (<5.0 kcal/mol, PM3).<sup>19</sup> With this in mind, we experimentally tested the formation of **13–17**<sub>out/in</sub> (Figure 7) by examining the coordination of **6** to different ligands **8–12** (Figure 8).

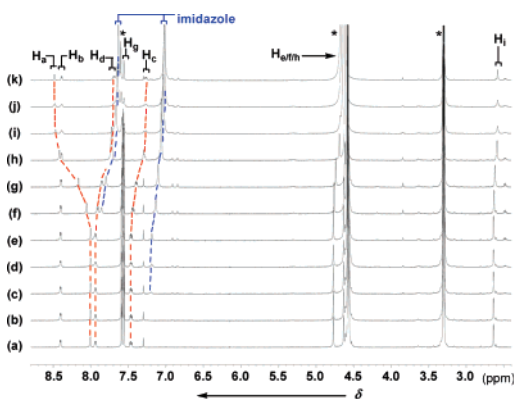


**Figure 7.** A series of <sup>1</sup>H NMR spectra of a 2.2 mM solution of **6** (500 MHz, CDCl<sub>3</sub>/CD<sub>3</sub>OD = 1:1, 300 K) recorded on addition of a standard solution of imidazole **8** (112.0 mM, CDCl<sub>3</sub>/CD<sub>3</sub>OD = 1:1) such that the final mixture comprises (a) 0, (b) 0.3, (c) 0.5, (d) 0.8, (e) 1.0, (f) 2.3, (g) 3.6, (h) 8.8, (i) 14, (j) 19, and (k) 24 mol equiv of imidazole.

On the basis of the results of <sup>1</sup>H NMR titrations and 2D DOSY measurements,<sup>10</sup> guests **8–11**, but not **12**, bind to **6** with variable affinity, leaving the solvated cavity “unoccupied”. Downfield <sup>1</sup>H NMR complexation-induced shifts (CIS)<sup>10</sup> of the guests were indicative of “outside” binding. The formation of [**13-out**] and [**15-out**], for example, was evident up until 1.5 or 0.5 mol equiv of imidazole (Figure 8) or azetidine, respectively, was added to a solution of **6**. The excess of the ligands, however, triggered additional equilibria wherein “free” polydentate **4** was formed.<sup>10</sup> In the cases of aziridine and thirane, the removal of silver from **6**

(19) Sheu, C.; Houk, K. N. *J. Am. Chem. Soc.* **1996**, *118*, 8056.

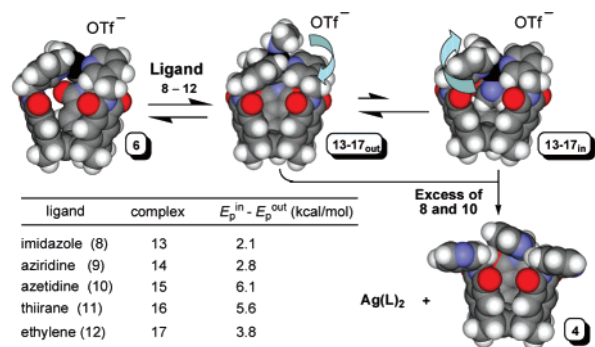


**Figure 8.** Energy-minimized conformations (DFT, BP86) of **6**, **14-out**, **14-in**, and **4**. DFT (BP86) calculated energy differences for **13–17** (in versus out).

was not observed, presumably due to the generally weaker affinity of these ligands toward the Ag(I) cation.<sup>20</sup>

Deliberate positioning of the fourth ligand in **6**, inside or outside of the cavity, and its regulation with an external stimulus can be of great interest if extra stabilization of a reactive intermediate is sought, or for manipulation of chemical reactivity that confined and dynamic environments can afford. Strategies developed in this study will further be used toward these goals, and the results will be reported in due course.

**Acknowledgment.** This research was financially supported by the Ohio State University. C.M.H. acknowledges financial support from the NSF. Generous computational resources were provided by the Ohio Supercomputer Center.

**Supporting Information Available:** Detailed descriptions of experimental methods and synthetic procedures. This material is available free of charge via the Internet at <http://pubs.acs.org>.

OL0705595

(20) (a) Edwards, J. O. *J. Am. Chem. Soc.* **1961**, *83*, 355. (b) Resika Dias, H. V.; Wang, Z.; Jackson, T. B. *Inorg. Chem.* **2000**, *30*, 3724.